The Variation in the Thermal Low-Pressure Location Index over the Qinghai–Tibet Plateau and Its Relationship with Summer

Xie qing Xia * , Mingfei Zhou , Yulei Zhu , Hongzhong Tang , Jing Yang , Qingbing Pang

Posted Date: 9 April 2024

doi: 10.20944/preprints202404.0681.v1

Keywords: Qinghai–Tibet Plateau; thermal low pressure; the location indexes; precipitation

Article

The Variation in the Thermal Low-Pressure Location Index over the Qinghai–Tibet Plateau and Its Relationship with Summer

Xie qing Xia *, Mingfei Zhou , Yulei Zhu , Hongzhong Tang , Jing Yang , Qingbing Pang

Posted Date: 9 April 2024

doi: 10.20944/preprints202404.0681.v1

Keywords: Qinghai–Tibet Plateau; thermal low pressure; the location indexes; precipitation

Article

The Variation in the Thermal Low-Pressure Location Index over the Qinghai–Tibet Plateau and its Relationship with Summer Precipitation in China

Qingxia Xie [1,*], MingFei Zhou [1], YuLei Zhu [1], HongZhong Tang [2], Jing Yang [1] and Qingbing Pang [1]

[1] Meteorological observatory of Guizhou province, Guiyang, 550002
[2] Qiannan Prefecture meteorological Observatory of Guizhou province, Duyun, 558000
* Correspondence: 66506485@qq.com ; Tel.: +86-15286002576

Abstract: Utilizing NCEP/NCAR monthly reanalysis data alongside precipitation observations from 1936 monitoring stations across China spanning from 1966 to 2022, this study establishes a location index for the thermal low-pressure center situated over the Qinghai–Tibet Plateau. Temporal variations in the location index and summer (July) precipitation patterns in China were studied. Over the past six decades, thermal low-pressure centers have been predominantly positioned near 90°E and 32.5°N on the plateau, with their distribution extending from east to west rather than from south to north. The longitudinal and latitudinal position indices exhibit contrasting linear trends, with a positive trend observed during the 1970s and early 21st century and a negative trend in subsequent decades. Mutation analysis highlights pronounced weakening mutations occurring in 1981 and 1973, with the longitudinal index transitioning from an inter-annual cycle of approximately 6-8 years, while the latitudinal index displays quasi-cyclic oscillations of 5 and 8 and 12-14 years. Strong negative correlations are evident between the location indices and precipitation along the southeastern edge of the Qinghai–Tibet Plateau and in Southern China, contrasting with the positive correlations observed in the central-eastern plateau, northwest China, North China, and the Huang-Huai region. The influence of southerly airflow predominates over much of China east of the plateau, while northwest China experiences convergence between northerly and southerly airflow. Higher location indices correspond to weaker surface cold air masses and strengthened Western Pacific Subtropical and South Asian Highs south of the Yangtze River Basin, resulting in significantly reduced rainfall in the southern Yangtze River region and increased rainfall in northwest China.

Keywords: Qinghai–Tibet Plateau; thermal low pressure; the location indexes; precipitation

1. Introduction

Known as the third pole of the earth, the Qinghai–Tibet Plateau is located in the central and southern parts of Asia. Its uplift has changed climate patterns in Asia [1]; its climate changes before that of the rest of China [2]. In the past 60 years, the Qinghai–Tibet Plateau has been the fastest-warming region in China, more than twice the global warming rate over the same period. The frequency of extreme high temperature and precipitation events has increased significantly. The Qinghai–Tibet Plateau has an important impact on circulations over and around it and influences climate change in China, and even the world. Therefore, the Qinghai–Tibet Plateau has attracted much attention. The thermal low pressure on the plateau plays an important role in affecting weather and climate downstream. However, at present, more attention is focused on plateau monsoons, plateau snow cover, etc., but less attention is paid to the thermal low pressure on the plateau.

Thermal low-pressure systems, characterized by shallow and relatively immobile warm air masses near the surface, are significant atmospheric features. Among the most extensively researched is the thermal low-pressure system of the Saudi Peninsula, which is primarily driven by boundary layer dynamics and underlying surface influences [3–6]. Beyond the thermal low-pressure phenomenon of the Qinghai–Tibet Plateau, China also experiences the southwest thermal low-

 doi:10.20944/preprints202404.0681.v1

pressure and southern Xinjiang thermal low-pressure systems [7,8]. Observations indicate that at 600 hPa, the Tibetan Plateau exhibits low pressures during summer and high pressures during winter [9]. By employing an intensity index to gauge the strength of the thermal low-pressure system over the Tibetan Plateau, Xie et al. [10] observed a general weakening trend in summertime low pressure over the Qinghai–Tibet Plateau spanning the last 62 years. Additionally, longitude and latitude indexes have been utilized to elucidate the east–west and north–south spatial variations in the southwest thermal low-pressure system's position [11,12]. These indexes, derived as averages across all stations within the thermal low-pressure study area, have facilitated discussions on the spatiotemporal distribution characteristics of the southwest thermal low-pressure system.

In China, the occurrence of extreme summer precipitation poses a significant threat to people, property, and the national economy, underscoring the urgent need for thorough investigations. Thermal low-pressure systems can sometimes trigger heavy rainfall [13–15]. However, due to the intricate interplay of dynamic and thermodynamic atmospheric processes on the plateau, research on summer rainfall induced by plateau thermal low pressure in China remains limited. Prior studies have suggested that the plateau's atmospheric heat sources serve as crucial indicators of summer precipitation in regions such as Jianghuai, South China, and North China [16–18]. Enhanced plateau heat sources correspond to increased precipitation in the upper reaches of the Yangtze and Huaihe River basins and decreased precipitation in southeast China and North China. The fluctuation in heat sources over the Qinghai–Tibet Plateau correlates closely with variations in thermal low-pressure intensity. Consequently, fluctuations in thermal low pressure over the plateau may lead to variations in summer precipitation across China. Specifically, during summers characterized by abnormally strong thermal low pressure over the Qinghai–Tibet Plateau, precipitation in the upper, middle, and lower reaches of the Yangtze River and the northwest region of the plateau experiences abnormal increases [9]. Conversely, precipitation totals are notably diminished in the western Sichuan Basin, the Hetao area, and North China. Furthermore, the intensification of plateau thermal low pressure typically results in increased precipitation in the Yangtze River Basin and Xinjiang, accompanied by reduced precipitation in northeast China, North China, southwest China, and South China, and vice versa [12].

Currently, there is a scarcity of research focusing on the thermal low-pressure system over the Qinghai–Tibet Plateau. Compounded by the region's complex terrain and limited observational data, there is a lack of standardized definitions for the circulation index utilized to characterize its active center. Addressing this gap, this paper proposes a method for defining a Qinghai–Tibet Plateau thermal low-pressure location index. Additionally, this study investigates the interannual and interdecadal variations in the thermal low-pressure location index over the Qinghai–Tibet Plateau. By analyzing the spatial and temporal variability of the thermal low-pressure system's location, this research aims to elucidate its relationship with summer precipitation patterns across China. Ultimately, the findings of this study aspire to provide a theoretical framework for enhancing summer precipitation forecasting capabilities in China.

2. Data and Methods

In this paper, the summertime (July) monthly mean height and wind field from the reanalyzed NCEP/NCAR data are used; the horizontal grid resolution is 2.5°×2.5°. Since there was no low-pressure center in the 600 hPa altitude field for many years in the main area of the plateau from 1948 to1965, we used data from 1966 to 2022. The monthly precipitation data from 1936 stations in China during summer (July) from 1966 to 2022 are also used. The main range of the Qinghai–Tibet Plateau is determined to be 27.5°～ 40°N and 80°～ 102.5°E. However, due to the difference between the model terrain used in the assimilation system and the real terrain, there may be certain limitations.

In terms of data selection, Bai Huzhi et al. [9] proved that the 600 hPa height of the NCEP/NCAR reanalysis data can be applied to plateau areas. Some researchers (Tang Maocang [19]; Qi Dongmei et al. [20]) also used these data to conduct plateau research. In addition, since 600 hPa is closer to the surface of the Qinghai–Tibet Plateau in summer, it is affected by surface heating on the Qinghai–Tibet Plateau, and this is a good representative of the plateau thermal low pressure. Therefore, the 600 hPa

 doi:10.20944/preprints202404.0681.v1

monthly average of the NCEP/NCAR reanalysis data is used to discuss the characteristics of Qinghai–Tibet Plateau thermal low pressure.

The definition of the position index of thermal low pressure is based on the definition of the polar vortex position index. Because the thermal low pressure is shallow and the range is relatively small, it is impossible to uniformly select a closed center line to determine the position of the center of low pressure in the long-term time series. Moreover, due to there being minimal variabilities in the geopotential height of the Qinghai–Tibet Plateau and the resolution of the data used (2.5°×2.5°), the lowest point of the thermal low-pressure center over the Qinghai–Tibet Plateau will be the same for many years in a row. Therefore, closed center lines of low pressure with the lowest values are selected for each year. When there are two or more centers with the same center value, the low-pressure center closest to the center of the plateau is selected. The mean longitude and latitude of all the grid points surrounded by the closed center line represent the longitude and latitude indexes of the central location index of plateau thermal low pressure, respectively. When the longitude and latitude indexes are high, this indicates that the central locations of the Qinghai–Tibet Plateau thermal low pressure are inclined to the east and north, respectively, and vice versa.

Some scholars define it as the average longitude and latitude of all stations in the closed pressure control area, but it will average out the real low center. There are also scholars who average the latitude and longitude of a certain characteristic contour in a specific region for many years, which will filter out some particularly weak or strong years. Therefore, the method used in the paper is convenient and reliable; however, the disadvantage of this method is that the workload is very large.

First, we use the Mann–Kendall method [21] and moving t-test [21] to discuss the mutations in the thermal low location index over time in the Tibetan Plateau, and we discuss their periodic variation using wavelet analysis [21]. Then, we calculated the correlation coefficients between the thermal low-pressure location index and atmospheric circulation to discuss the dynamic mechanisms.

2.1. Mann–Kendall Method

The Mann–Kendall method [21] is a non-parametric statistical test method that can detect not only the change in a sequence, but also the turning points in a sequence. For the time series $x_1, x_2, \ldots, x_n$, S_k represents the cumulative count of the sample xi greater than x_j ($1 \le j \le i$). Under the assumption of independence of random time series, we define UF_k as follows:

$$UF_k = [S_k - E(S_k)]/\sqrt{var(S_k)} \qquad k = 1, 2, \ldots, n \tag{1}$$

Here, $UF_1 = 0$, and $E(S_k)$, $var(S_k)$ are the mean and variance of the cumulative counts, respectively; they are calculated as follows:

$$E(S_k) = n(n-1)/4 \tag{2}$$

$$var(S_k) = n(n-1)(2n+5)/72 \tag{3}$$

Given the significance level α, $U\alpha$ represents a normal distribution. If $|UF_i| > U\alpha$, this indicates that there is an obvious change in the sequence. In the reverse order of time series x, $x_n, x_{n-1}, \ldots, x_1$, we repeat the above process, while ensuring that $UB_k = -UF_k$ ($k = n, n-1, \ldots, 1$), $UB_1 = 0$. We drew a graph of UB_k and UF_k. If the two curves intersect, and the intersection is between the critical boundary, then the time corresponding to the intersection represents the time at which the mutation begins.

2.2. Wavelet analysis

Wavelet analysis is also known as multi-resolution analysis, and this is considered to be a breakthrough in Fourier analysis methods.

According to the time scale of this research problem, the initial value of the frequency parameter a and the time interval for the growth of a are determined.

Then, we calculate the generating wavelet function.

$$\Psi(t) = (1-t^2)(1/\sqrt{2\pi})e^{\frac{-t^2}{2}} \qquad -\infty < t < \infty \tag{4}$$

 doi:10.20944/preprints202404.0681.v1

Next, we combine the determined frequency a, the study object sequence f(t) and the mother wavelet function $\Psi(t)$ in Formula (2) to calculate the wavelet change.

$$\omega_f(a, b)=|a|^{-1/2}\Delta t \sum_{i=1}^{n} f(i\Delta t)\Psi(\frac{i\Delta t-b}{a}) \quad (5)$$

3. Results

3.1. The Variation Characteristics of the Thermal Low Location Index over the Qinghai–Tibet Plateau

Figure 1 shows the distribution of the location of the center of summer thermal low-pressure events during 1966-2014. The centers were mainly located around 90°E and 32.5°N within a geopotential height of 4360 gpm, and the distribution extended more significantly from east to west than it did from south to north. There was no thermal low-pressure center in the main area of the plateau in 1994 and 1997, and we chose locations with the lowest geopotential height in the main area of the Qinghai–Tibet Plateau.

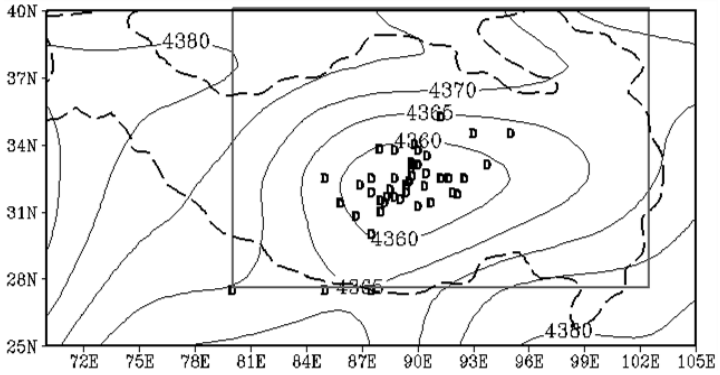

Figure 1. The figure shows the distribution of the thermal low center locations in summer (July) during 1966–2022（the thick solid line denotes the range of Qinghai–Tibet Plateau; thick dashed line denotes 3000 m topographical isoline of the Qinghai–Tibet Plateau; and D represents the thermal low center locations.)

The longitude index presents an overall linear downward trend with a coefficient of -0.023 (Figure2a), while the latitude index presents a downward trend before the 21st century and an upward trend after the 21st century. The trend coefficient is 0.013 (Figure2b). The decline of the longitude index indicates that the Qinghai–Tibet Plateau thermal low-pressure center has gradually moved westward over the last 60 years, while the latitude index moved southward before the 21st century. Thus, the thermal low-pressure center moved southwestward during this period before the 21st century, which corresponds with the research on the plateau heat source mentioned by Feng Song [22], Wei Zhigang et al. [23] and Hu Jun et al. [24]. The warming trend in the southwest is significantly stronger than that in the east. But since the beginning of the 21st century, these two indices have begun to move east and north, so the low-pressure center is moving northeastward.

 doi:10.20944/preprints202404.0681.v1

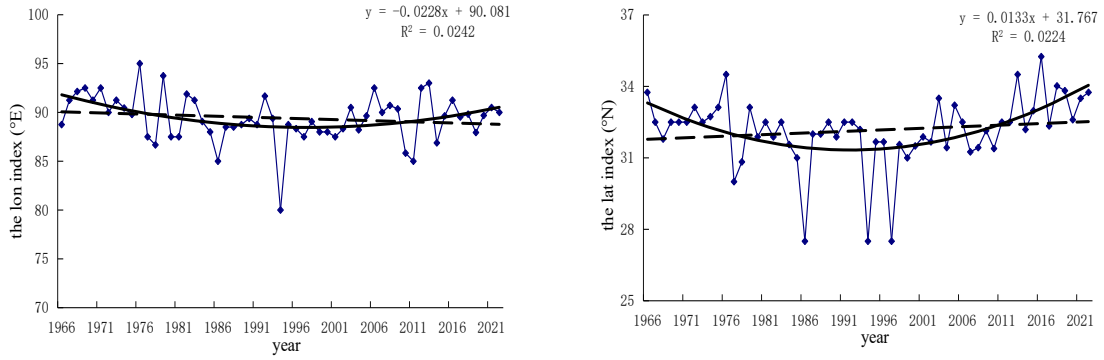

(**a**) (**b**)

Figure 2. Interannual variation in the longitude (a) and latitude indexes (b) of the Tibetan Plateau in summer (July) 1966-2022 (the thin line). Polynomial fitting line (solid thick line); linear trend (dashed line).

In order to further explore the decadal variation in Qinghai–Tibet Plateau thermal low pressure, we calculate this anomaly for each decade (Table 1).

The longitude and latitude location indexes of Qinghai–Tibet Plateau thermal low pressure were positive in the 1970s and 2010s, indicating that they were high (northeast) during these periods, while they were negative in the 1980s and 1990s, indicating that the low-pressure location indexes were low (southwest) during these periods. The longitude and latitude indexes had the largest absolute negative values in the 1990s, indicating that thermal low pressure was positioned more southwesterly in this era. The longitude index reached its maximum positive value in the 1970s, while the latitude index reached its maximum positive value in the 2010s, indicating that Qinghai–Tibet Plateau thermal low pressure was positioned significantly more northeasterly than it had been during the rest of this period. The same conclusion can be drawn from the polynomial fitting curve in Figure 2. It can be seen that from the late 1970s to the early 1980s, the decadal variation in the longitude and latitude indexes of the Qinghai–Tibet Plateau thermal low pressure suddenly changed from high to low, so the mutation time and cycle are discussed below.

Table 1. Interdecadal anomalies in the longitude and latitude location indexes over the Qinghai–Tibet Plateau in summer (July) during 1966-2022.

years	Anomaly(lon)	Anomaly(lat)
1970-1979	**1.5748**	**0.4478**
1980-1989	**-0.6472**	**-0.5122**
1990-1999	**-1.1592**	**-1.0472**
2000-2009	**0.3338**	**0.0068**
2010-2019	**-0.1022**	**1.1048**

The negative curves of the longitude index (Figure3a) from the 1970s to the early 1980s and in the late 2010s were greater than 0, and the latitude index (Figure3b) from the late 1960s to the early 1970s indicates an exponential upward trend. There was a significant downward trend before the 21st century, and the trend from the mid-1990s to the early 21st century exceeded the 95% confidence level. At the beginning of the 21st century, there was a significant upward trend again, which was consistent with the analysis of the time series anomaly. The positive and negative series of the longitude index intersected in 1981, 2015, 2017, 2020 and 2021, while the positive and negative curves of the latitude index intersected in 1973, 2021 and 2022. However, sliding T-test analysis confirmed that the 1981 intersection of the longitude index represents climate change, while the 1973 intersection of the latitude index represents climate change.

 doi:10.20944/preprints202404.0681.v1

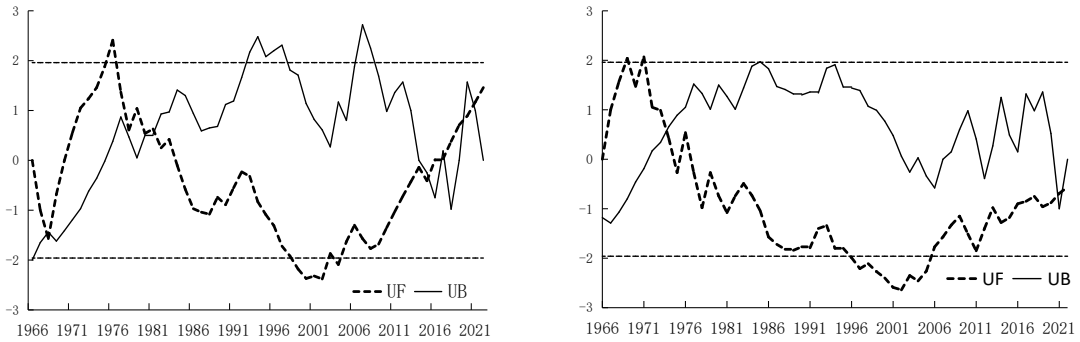

Figure 3. M-K mutation for the longitude（a）and latitude indexes (b) on the Qinghai–Tibet Plateau in summer (July) during 1966-2022 (the transverse dashed lines indicate the critical value at the confidence level of 95 %, the solid line is a location sequence, and the dashed line is a negative sequence.).

Morlet wavelet transform can further show the temporal change in longitude and latitude location indexes of the Qinghai–Tibet Plateau thermal low pressure in the last 60 years. The cycle of the longitude index (Figure 4a) grew slightly before the 1990s and then stabilized at about 8 years. The longitude index had an interdecadal cycle of about 18 years, but it has gradually increased since the early 21st century. The 6–8-year cycle passed the 90% confidence test in the late 1970s through the early 21st century. However, the latitude index (Figure 4b) had two interannual cycles of 5 and 8 years; the former was mainly assigned to the late 1990s, and it has a gradually shortened trend. The latter increased to about 12 years in the 1990s and then basically stayed the same at about 14 years. The 5-year cycle passed the 90% confidence test from the 1970s to the late 1990s, and the 8-14-year cycle passed the 90% confidence test from the late 1970s to the early 21st century.

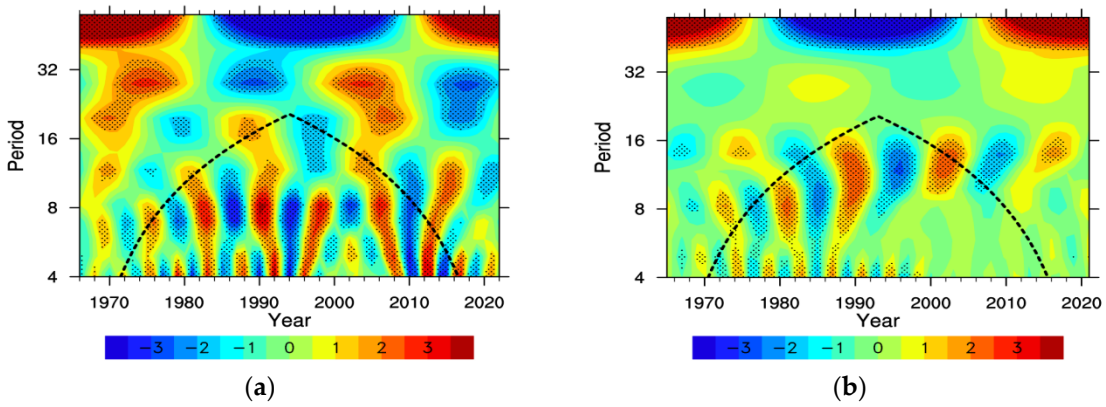

Figure 4. The Morlet wavelet real part of the lon (a) and lat indexes (b) in summer (July) during 1966-2022.

3.2. The Relationship between Qinghai–Tibet Thermal Low Pressure and Summer Precipitation and Atmospheric Circulation in China

We analyze the correlation between the longitude and latitude location indexes of Qinghai–Tibet Plateau thermal low pressure and the monthly precipitation data of 1936 stations in China, alongside the U and V wind fields of the 850 hPa, 1000 hPa, 500 hPa, and 100 hPa height fields from 1966 to 2022. Then, the years with high and low Qinghai–Tibet Plateau thermal low-pressure location indexes are selected for analysis. When the inter-annual variation in location index is one times larger (or one time smaller) than the mean variance, this year represents a low (or high) low-pressure position index. The years in which the longitude index is higher are 1968, 1969, 1971, 1976, 1979, 1982, 1992, 2006, 2012, and 2013. The years featuring a low longitude index are 1978, 1986, 1994, 2010, 2011, and

 doi:10.20944/preprints202404.0681.v1

2014. The years with a high latitude index are 1966, 1976, 2013, 2016, 2018, 2019, and 2022, while the years with a low value are 1977, 1978, 1986, 1994, and 1997. The summer precipitation value, an 850 hPa wind field, and the 1000 hPa, 500 hPa, and 100 hPa height fields in the years with a high/low-pressure index were, respectively, synthesized to create difference plots (values in all the high-index years minus those of the low-index years) (figure omitted); these were then compared with the correlation coefficient plot

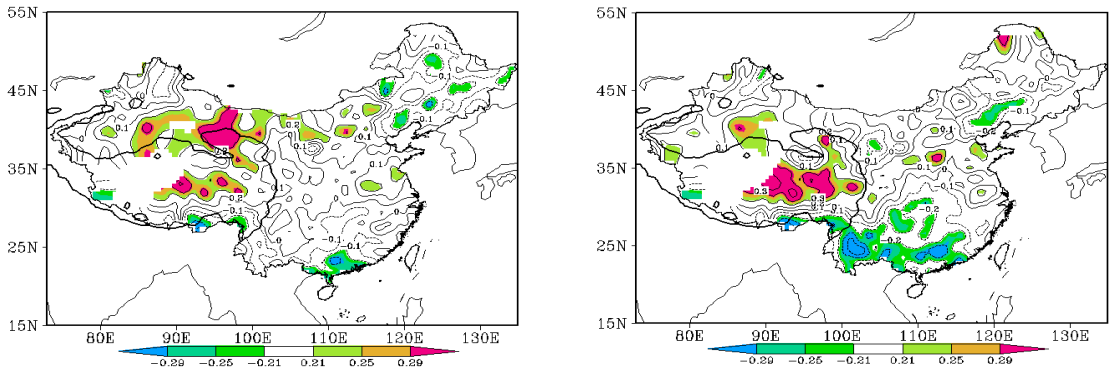

Figure 5. Correlations between the longitude (a) and latitude indexes (b) with summer (July) precipitation during 1966-2022. The shaded areas represent those where the T-test passed the 90%, 95%, and 99% significance levels.

The longitude index and precipitation (Figure 5a) were negatively correlated in the northwest of Xinjiang, the southeastern edge of the Qinghai–Tibet Plateau, the southern part of southwest China, the central part of South China, and most of the northeast regions. Among them, the southeastern edge of the Qinghai–Tibet Plateau and the southern and eastern parts of South China are the most significant, and the absolute value of the T-test was above 0.21, passing the 90% reliability test. There was a positive correlation between most of the northwest region and most of the Qinghai–Tibet Plateau region and east of the Huanghuai coastal region. The correlation between the Qinghai–Tibet Plateau and northwest region passed the 90% reliability test.

The correlation between the latitude index and rainfall (Figure 5b) is almost the same as that of the longitude index, except that most of the southwest region has a negative correlation, and the relationship is as significant as that in Central China. The north of the northeast region has a minor positive correlation with the northwest area, while the central and eastern parts of the Qinghai–Tibet Plateau and the Huanghuai area have larger correlation values. These results show that when the thermal low pressure is located in the east or north (west or south) of the Qinghai–Tibet Plateau, the level of precipitation over the southeastern edge of the Qinghai–Tibet Plateau, South China, Central China and the south and northeast parts of China is significantly lower/higher. The level of precipitation is higher/lower in most parts of northwest China, most of the plateau and to the east of the Huang-Huai coastal areas. When thermal low pressure is located farther north, the amount of precipitation is lower, and vice versa. The map showing the difference in years with high and low location indexes is basically consistent with the correlation coefficient, indicating that less precipitation occurred in the years with high longitude and latitude indexes than that in the years with low values from the southeastern edge of the Qinghai–Tibet Plateau to South China. In the eastern and northern parts of the Qinghai–Tibet Plateau, more precipitation occurred in the years with high longitude and latitude indexes than that in the years with low values. This shows that the high and low Qinghai–Tibet Plateau thermal low position indexes in this paper are reliable.

3.3. Geopotential Height at 1000 hPa

Due to the thermal difference between the ocean and land, a change in sea level pressure is very important for predicting summer precipitation. Therefore, the changes in the longitude and latitude indexes of Qinghai–Tibet Plateau thermal low pressure and sea-level pressure are compared and

 doi:10.20944/preprints202404.0681.v1

analyzed here. The distribution of the correlation coefficients of the longitude and latitude indexes of Qinghai–Tibet Plateau thermal low pressure at the 1000hPa height are very similar (Figure 6a). Except for the eastern margin of northeast China, the Indian Ocean, the South China Sea and the West Pacific region, most of the other regions are negatively correlated. The central and eastern parts of northwest China, the central and eastern parts of the Qinghai–Tibet Plateau and the northern parts of southwest China pass the 90% reliability test, indicating that the higher the index is (thermal low pressure is located further north and east), the lower the pressure is in most of China, the weaker the cold air is, the higher the temperature is, the more there energy is, and the more conducive these conditions are to short-term heavy rainfall.

When the longitude index of thermal low pressure on the Qinghai–Tibet Plateau was high (Figure 6b), most of the country was controlled by low pressure. The Mongolia low-pressure system was located at the junction of southern Mongolia and Inner Mongolia, with a central intensity of 20 gpm, and two centers were located in central China and Xinjiang, respectively. The Mongolian low-pressure system was located in only two east–west centers in Xinjiang and Inner Mongolia. However, in the low-value years in the two areas (figure omitted), the Mongolian low-pressure system was weak. The chart showing the difference in summertime sea-level pressure in the high- and low-value years is basically consistent with the correlation coefficient (figure omitted) and is also consistent with the analysis results of the precipitation mentioned above.

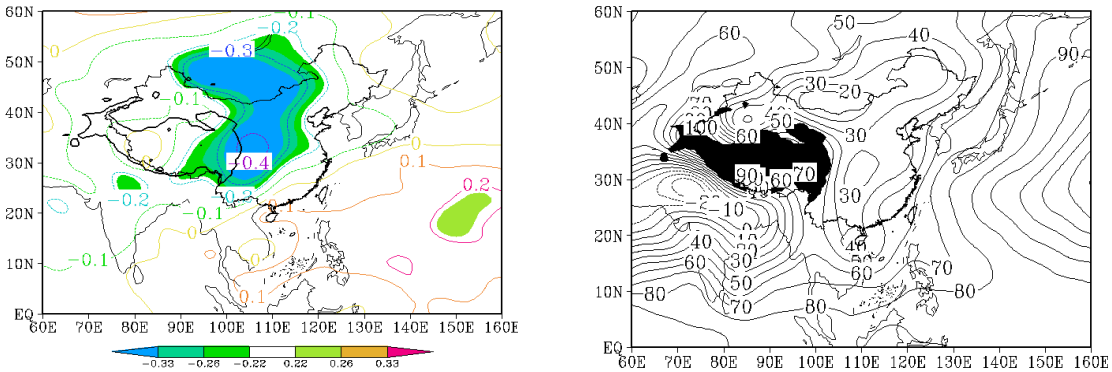

Figure 6. The figure shows the correlation coefficient (a) of the longitude index of the Qinghai–Tibet Plateau thermal low pressure and 1000hPa height field. The 1000hPa height field of the longitude index in high-value years (b) in the summer (July) during 1966～2022. The shaded areas represent those where the correlation passes the 90%、95%, and 99% significance levels.

3.4.850. hPa Wind Field

The longitude (Figure 7a) and latitude indexes (Figure omitted) are basically consistent with the correlation coefficient diagram of 850hPa wind field distribution in the summer. There is a strong cyclone in central Mongolia; a southeasterly air flow in the southern part of the Pacific anticyclone passes over the South China Sea and is divided into two branches over the Indo-China Peninsula, one of which moves northward from South China, along with western air flow in the northern part of the Bay of Bengal. In the eastern part of northwest China, it meets the northwesterly air flow from the Arctic Ocean; this meets the water vapor condition for more precipitation in northwest China and the east part of the Qinghai–Tibet Plateau, while there is less rain in the coastal area of South China. This is consistent with the conclusion obtained by He Jinhai et al. [25]. The other flow joins the Bay of Bengal air flow. In northeast China and North China, southerly and southeasterly ageostrophic winds prevail, and the cold air activity in the north is weak in summer when the plateau low-pressure index is high, so there is less precipitation in most parts of northeast China.

In the years with high longitude and latitude indexes (Figure 6b), the southern Arabian Sea is controlled by a strong westerly air flow, which passes over the Indian Peninsula and the Bay of Bengal, and then arrives at South China and the South China Sea; a part of the flow continues eastward through the Philippines to join with the southeasterly air flow south of the West Pacific

 doi:10.20944/preprints202404.0681.v1

subtropical high-pressure system, and a part of this flows directly northward from South China and arrives at the central and eastern parts of China. A cyclone forms in west–central Mongolia, while the anticyclone ridge in the Pacific Ocean is at 40N, with a strong intensity. In the years with low latitude and longitude indexes, the northbound air flow over South China is markedly weaker; there is only one cyclone in central Mongolia, and the Pacific anticyclone air flow is also markedly weaker. The plot showing the difference in the years with high and low latitude and longitude indexes is very similar to the correlation coefficient plot.

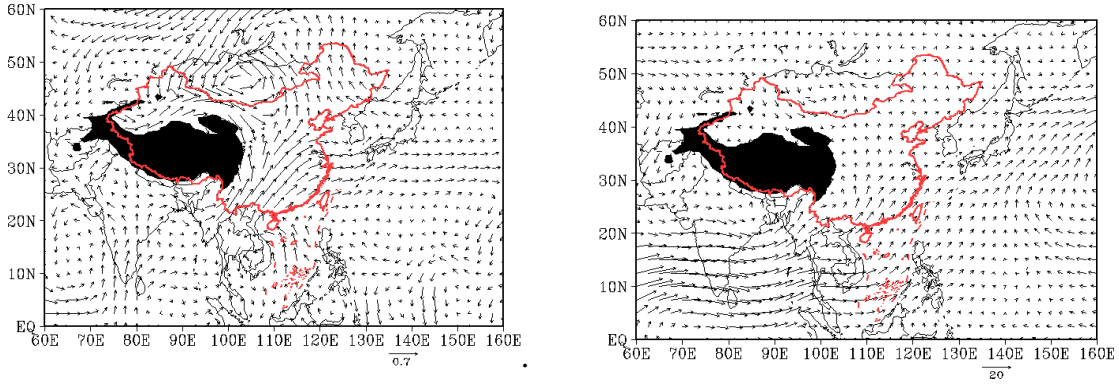

(**a**) (**b**)

Figure 7. The figure shows the correlation coefficient (a) of the longitude index of the Qinghai–Tibet Plateau thermal low pressure and 850hPa wind field. The 850hPa wind field of the longitude index in high-value years (b) in the summer (July) during 1966～2022.

3.5. The 500 hPa Height Field

The changes in the movement and intensity of various weather systems at 500 hPa, such as the western Pacific subtropical high, upper trough and blocking high-pressure systems at the middle and high latitudes, have important effects on summer precipitation in China. As can be seen from the correlation coefficient chart (Figure 8a), there is a positive correlation in South China and a negative correlation in most of the other regions. Between 30°N and 50°N, the main positive correlation centers are located in Xinjiang, the Qinghai–Tibet Plateau and Japan, and the correlation between the longitude index and the 500 hPa height of this region passed the 90% significance level. These results show that the geopotential height in the middle and high latitudes decreases when the longitude and latitude indexes are high, while the geopotential height in the south of the Yangtze River Basin, the South China Sea and the West Pacific Ocean increases, and vice versa.

The ridge at 588 dagpm of the western Pacific subtropical high-pressure system is around 30°N, and the western ridge point does not exceed 120°E in the years with a high longitude index (Figure 8b) or 130°E in the years with a high latitude index. The Indian low-pressure system has only a large center of 584 dagpm in the years with a high longitude index, while no closed center formed in the years with a high latitude index. In the years with low longitude and latitude location indexes (figure omitted), the western Pacific subtropical high-pressure system is markedly weaker; the Yangtze River basin represents a trough area of low pressure, the Indian low-pressure system has a smaller range, and the center is located more easterly. The map showing the difference (figure omitted) is similar to the correlation coefficient map, indicating that in the years with high longitude and latitude location indexes, the position of the western Pacific subtropical high-pressure ridge is located more to the west of the north than usual, and a summer monsoon mainly affects the area north of the Yangtze River, resulting in more precipitation there.

Preprints.org (www.preprints.org) | NOT PEER-REVIEWED | Posted: 9 April 2024 doi:10.20944/preprints202404.0681.v1

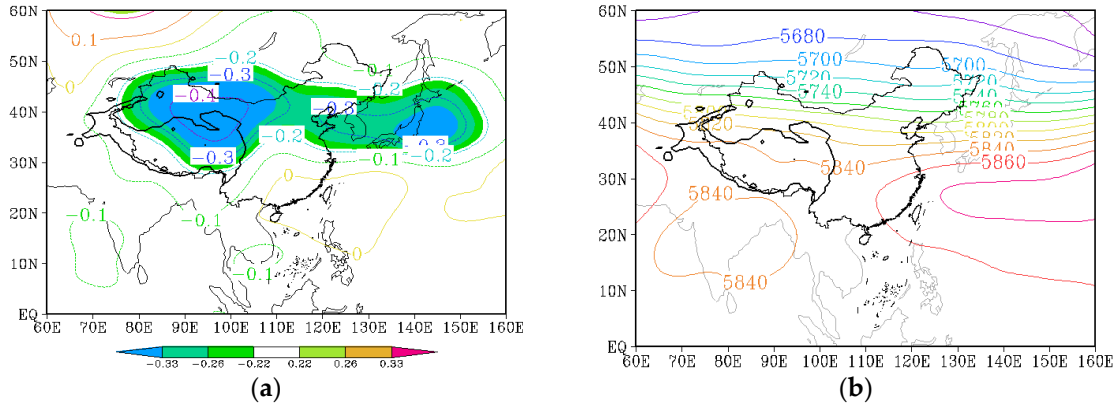

Figure 8. The figure shows the correlation coefficient (a) of the longitude index of the Qinghai–Tibet Plateau thermal low pressure and 500hPa height field. The 500hPa height field of the longitude index in high-value years (b) in the summer (July) during 1966～2022. The shaded areas represent those where the correlation passes the 90%,95%, and 99% significance levels.

3.6.100. hPa Height Field

The timing and intensity of the South Asian high-pressure system ascending toward the Qinghai–Tibet Plateau, as well as its east–west oscillation and southward and northward movements [26–28], have an important impact on the summer precipitation in China. The formation of the South Asian high-pressure system is closely related to Qinghai–Tibet Plateau heating [29,30]. The correlation coefficient (Figure 9a) diagram shows that the latitude and longitude indexes are negatively correlated with the geopotential height in Xinjiang, most of the Qinghai–Tibet Plateau, northwest China, northeast China and Japan, but are positively correlated with central and southern China.

In the years with high longitude (Figure 9b) and latitude indexes, the center of the South Asian high-pressure system is located in the Iranian Plateau, with a central intensity of 1686 dagpm, which extends more eastward to the central part of the Qinghai–Tibet Plateau compared with that during the low-value years. The feature line at 1680 dagpm ranges from 24°N to 40°N, and the eastern ridge point is near 110°E. Tao Shiyan et al. [31] pointed out that the 100 hPa flow pattern in southern Asia and the 500 hPa western Pacific subtropical high-pressure system in summer have a trend of "moving in the same direction and moving away from each other". The diagram showing the difference (figure omitted) is similar to the correlation coefficient diagram, indicating that the eastward expansion and southward shift of the southern pressure and high-pressure systems resulted in increased summer precipitation in the Yangtze River Basin and its northern regions, while less summer precipitation occurred in South China and North China, which is consistent with Hu Jinggao et al. [31], who pointed out that "the east ridge of the South Asia High pressure is eastward, the Jianghuai River Basin has positive precipitation anomalies, and the southeast coast and South China have negative precipitation anomalies".

 doi:10.20944/preprints202404.0681.v1

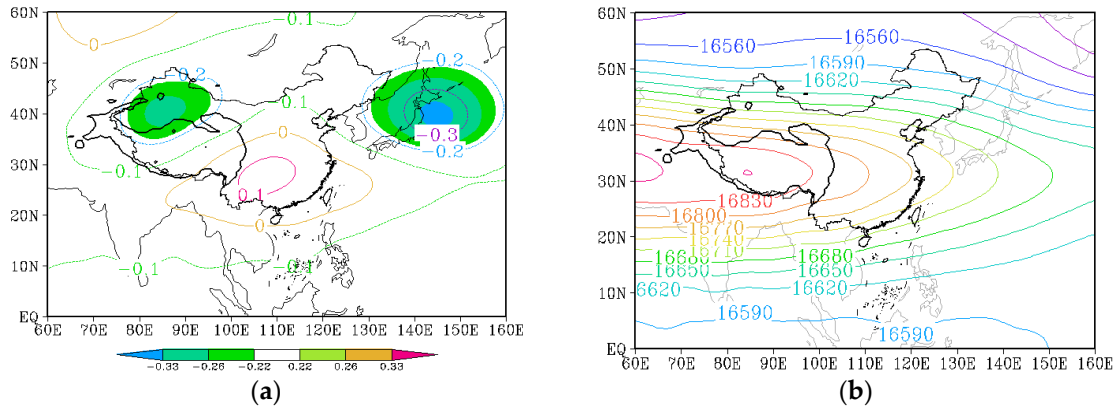

Figure 9. The figure shows the correlation coefficient (a) of the longitude index of the Qinghai–Tibet Plateau thermal low pressure and 100hPa height field. The 100hPa height field of the longitude index in high-value years (b) in the summer (July) during 1966～2022. The shaded areas represent those where the correlation passes the 90%, 95%, and 99% significance levels.

4. Conclusions

This study investigates the characteristics of the Tibetan–Qinghai Plateau thermal low-pressure system's location changes and its impact on summer precipitation patterns in China. The key findings are summarized as follows:

(1) Over the past six decades, the thermal low-pressure centers over the Qinghai–Tibet Plateau have predominantly positioned near 90°E and 32.5°N. Notably, the distribution area has exhibited more significant expansion from east to west compared to from south to north.

(2) Analysis of the longitude and latitude indexes reveals a linear decline and an upward trend, respectively. Anomalies were positive in the 1970s and early 21st century but turned negative in subsequent years. Abrupt changes occurred in 1973 and 1981, transitioning from higher to lower values. The longitude index exhibits 6-8-year quasi-periodic oscillations, while the latitude index displayed 5-year and 8-year interannual oscillations before the 1990s and gradually shifted to 12-14-year interdecadal oscillations.

(3) The indexes exhibit inverse correlations with precipitation from the southeastern edge of the Qinghai–Tibet Plateau to the southern Yangtze River and northeast region. However, they are significantly positively correlated with precipitation from the central-eastern region of the plateau to the northwest, North China, and the Huang-Huai region.

(4) Higher index values coincide with weaker ground-level cold air, leading to the predominance of southerly airflow over most of China east of the Qinghai–Tibet Plateau, while northwest China experiences a convergence of northerly and southerly airflow. Moreover, the western Pacific subtropical high- and South Asian high-pressure systems south of the Yangtze River Basin strengthen, resulting in markedly increased rainfall in the south of the Yangtze River and northwest China.

Wang Xin et al.[32] found that "there are three main moving paths of low vortex on the plateau: northeast, southeast and east, among which the number of low vortex moving to northeast is the largest." "When the low vortex moves out of the plateau, there are two main paths: one is the northeast path, which mainly moves to Hexi, Ningxia and the Loess Plateau; The other is the southeast path, which mainly moves to the vicinity of Sichuan Basin, among which, the low vortex moving to the Loess Plateau is the most ", so whether the plateau thermal low-pressure center generated in the northeast direction in the 21st century is more conducive to its northeast movement? What is the development mechanism between them? The further analysis of these physical mechanisms is the focus of further efforts in the future.

Thanks are given to Professor Fan Guangzhou of the Chengdu University of Information Technology for his careful guidance, Zhao Zhenguo from the National Meteorological Center, and Wang Panxing from Nanjing University of Information Science and Technology for the helpful discussion.

 doi:10.20944/preprints202404.0681.v1

Author Contributions: Conceptualization, Q.X.; methodology, Q.X.; software, Q.X.; validation, Q.X.; formal analysis, Q.X.; investigation, Q.X.; resources, Q.X.; data curation, M.Z.; writing—original draft preparation, Q.X.; writing—review and editing, Q.P.; visualization, Y.Z.; supervision, H.T.; project administration, Q.X.; funding acquisition, J.Y. All authors have read and agreed to the published version of the manuscript.

Funding: This work was funded by Application of machine learning to high spatio-temporal resolution precipitation forecast in complex mountainous area of Guizhou Province (The Guizhou family supports [2023] General 235), Fengyun Satellite Application Initiative (2023) (FY-APP-ZX-2023.01), Demonstration study on key technologies for monitoring and forecasting of thunderstorms and gales in central Guizhou urban agglomeration (Guizhou family support [2023] General 236).

Institutional Review Board Statement: Not applicable.

Informed Consent Statement: Not applicable.

Data Availability Statement: NCEP/NCAR reanalysis I data provided by the NOAA PSL, Boulder, CO, USA, from their website at https://psl.noaa.gov (accessed on 10 March 2023). The precipitation data provided by the National Data Center for Meteorological Sciences of China, from their website at http://data.cma.cn/ (accessed on 10 March 2023).

Conflicts of Interest: The authors declare no conflicts of interest.

References

1. Wu G X.; Liu Y M.; Liu X. How the heating over the Ti2betan Plateau affects the Asian climate in summer [J]. Chinese J Atmos Sci (in Chinese) , 2005, 29 (1) : 47-56.
2. Zhang Y C.; Qian Y F. Numerical studies on the effects of the critical height of Qinghai-Xizang Plateau uplift on the atmosphere [J].Acta Meteor Sinica (in Chinese) 1999, 57(2): 157-167.
3. Blake D W.; Krishnamurti T N.; Low-Nam S V. Heat Low Over the Saudi Arabian Desert During May 1979(Summer MONEX) [J]. Monthly Weather Review, 1983, 111(9): 1759-1775.
4. Smith E A. The Structure of the Arabian Heat Low Part I: Surface Energy Budget [J]. Monthly Weather Review, 1986, 114(6): 1067-1083.
5. Smith E A. The Structure of the Arabian Heat Low Part II: Bulk Tropospheric Heat Budget and Implications [J]. Monthly Weather Review, 1986, 114(6):1084-1102.
6. Saad M. Impact of Shortwave Radiative Effects of Dust Aerosols on the Summer Season Heat Low over Saudi Arabia [J]. Monthly Weather Review, 1998, 126(12): 3153-3168.
7. Yang J.; Wang C.; LeI Y.; Genesis, Development and Struture Characteristics of Southwest Heat Low in spring [J]. Meteorological monthly, 2013, 39(02): 146-155.
8. Zhang Y Z.; Zhao Y.; Huo W.; Analysis on the characteristic of Heat Low in Summer over the Tarim Basin [J]. Journal of Chengdu University of Information Technology, 2023, 38(02): 214-220. DOI:10.16836/j.cnki.jcuit.2023.02.013.
9. Bai H Z.; Ma Z F.; Dong C J. Relationship between Qinghai-Xizang Plateau Region monsoon features and abnormal climate in china [J]. Journal of applied meteorological science, 2005, 16(4) : 484-491.
10. Xie Q X.; Fan G Z.; Zhou D W. Interannual and Interdecadel Changes of Summer Low over the Qinghai - Xizang Plateau and Its Relationship to Precipitation in China [J]. Plateau meteorology, 2012, 31 (6) : 1503-1510.
11. Xiong F.; Wang Y. The Research on the typical high impact weather system of Thermal Depression in southwest I [J]. Journal of tropical meteorology, 2008, 24(4) : 391-398.
12. Zhou C P. Pacific Warm pool and its influence: Relationship with EL Nino, Western Pacific Subtropical high, precipitation in China and natural disasters along China's coast [M]. Beijing: China Meteorological Press, 2001: 22-50.
13. Zhu Y Q.; Gao Q S.; Huang W G. Heavy rain forecast of thermal low pressure filling in Southwest China [J]. Guizhou Meteorology, 1994, 18 (2) : 5–121.
14. Ding Y H. Advanced Synoptics [M], Beijing: China Meteorological Press, 2005.
15. Eric A S. The Structure of the Arabian HeatLow PartI: Surface Energy Budget [J]. Monthly Weather Review, 1986, 114 (6) : 1067–1083.
16. Zhao P.; Chen L X. Climate characteristics of Qinghai2TibetPlateau atmospheric heat source in 35 years and its relation to Chi2nese precipitation [J]. Chinese Sci (D) (in Chinese), 2001, 31(4): 327-332.
17. Zhao P.; Chen L X. Interannual variability of atmospheric heat source/ sink over the Qinghai Xizang (Tibetan) Plateau and its relation to circulation [J]. Adv Atmos Sci, 2001, 18 (1): 106-116.
18. Bai J Y.; Xu X D.; Zhou Y S. A preliminary study on the influence of sensible heat anomaly over Qinghai-Tibet Plateau in spring on summer precipitation in the middle and lower reaches of Yangtze River [J]. Journal of Applied Meteorology, 2003, 14 (3) : 363-368.

 doi:10.20944/preprints202404.0681.v1

19. Tang M C. Interannual oscillation of plateau monsoon and its causes [J]. Scientia Meteorologica Sinica, 1995, 15 (4) : 64-68.
20. Qi D M.; Li Y Q.; Bai Y Y.; De Q. Definition and characteristic analysis of plateau summer monsoon index [J]. Research on Plateau and mountain Meteorology. 2009, 29 (4) : 001-009.
21. Wei, F. Modern Climate Statistical Diagnosis and Prediction Technology; 2nd ed.; China Meteorological Press: Beijing, China, 2007.
22. Feng S. Comprehensive Analysis and Causes of ten-thousand-year scale climate Change over the Tibetan Plateau [J], Ph. D. Thesis, Lanzhou Institute of Plateau Atmospheric Physics, Chinese Academy of Sciences, 1999, 11-23.
23. Wei Z G.; Huang R H.; Dong W J. Interannual and interdecadal variations of temperature and precipitation over the Tibetan Plateau, Chinese Journal of Atmospheric Sciences, 2003, 27 (2), 157-170.
24. Hu J.; Du J.; Bian D, et al. Interannual and interdecadal variations of Ground temperature in Tibet, Acta Geographica Sinica, 2007 (in Chinese).
25. He J H.; Liu Y Y.; Chang Y. Characteristics of summer precipitation anomalies and water vapor transport and circulation in Northwest China [J], Arid Meteorology, 2005, 23 (1) : 10-15.
26. Liu X.; Li W P.; Xu H X, et al. Effect of heating over the Tibetan Plateau on summer precipitation over East Asia [J]. Plateau Meteorology, 2007, 26(6) : 1287-1292.
27. Sun G W.; Song Z S. The establishment of South Asia High and its relationship with the evolution of atmospheric circulation and rain belt in China [C]. Influence of Qinghai-Tibet Plateau on weather in China in summer half year. Beijing: Science Press, 1987: 93-100.
28. Zhang J E. North-South movement of high pressure ridge in South Asia and Meiyu [C]. Influence of Qinghai-Tibet Plateau on weather in China in the Summer half year. Beijing: Science Press, 1987: 101-105.
29. Zhang Q.; Wu G X. The relationship between drought and flood in the Yangtze River Basin and South Asian High [J]. Acta Meteorologica Sinica, 2001, 59(5) : 569-577.
30. Liu M.; Hu L L.; Pu M J, et al. Evolution of South Asia high in summer and related weather systems [J]. Scientia Meteorologica Sinica, 2007, 27(3) : 294-301.
31. Tao S Y.; Zhu F K. The change of 100 millibar flow pattern in southern Asia in summer and its relationship with the ebb and flow of the Western Pacific subtropical high. Acta Meteorologica Sinica, 1964, 34 (4) : 385-396.
32. Wang X, LI Y Q, Yu S H et al. Statistical Study on the Plateau Low Vortex Activities [J]. Plateau meteorology, 2009, 28(01): 64-71.